

Kent Academic Repository

Full text document (pdf)

Citation for published version

Key, Alastair J. M. and Young, Jesse and Fisch, Michael and Chaney, Morgan and Kramer, Andrew and Eren, Metin I. (2018) Comparing the use of meat and clay during cutting and projectile research. *Engineering Fracture Mechanics*, 192 . pp. 163-175. ISSN 0013-7944.

DOI

<https://doi.org/10.1016/j.engfracmech.2018.02.010>

Link to record in KAR

<http://kar.kent.ac.uk/65898/>

Document Version

Author's Accepted Manuscript

Copyright & reuse

Content in the Kent Academic Repository is made available for research purposes. Unless otherwise stated all content is protected by copyright and in the absence of an open licence (eg Creative Commons), permissions for further reuse of content should be sought from the publisher, author or other copyright holder.

Versions of research

The version in the Kent Academic Repository may differ from the final published version.

Users are advised to check <http://kar.kent.ac.uk> for the status of the paper. **Users should always cite the published version of record.**

Enquiries

For any further enquiries regarding the licence status of this document, please contact:

researchsupport@kent.ac.uk

If you believe this document infringes copyright then please contact the KAR admin team with the take-down information provided at <http://kar.kent.ac.uk/contact.html>

1
2
3
4
5
6
7
8
9
10
11
12
13
14
15
16
17
18
19
20
21
22
23
24
25
26
27
28
29
30
31
32
33
34

Comparing the use of meat and clay during cutting and projectile research

Alastair Key* ^{1,2}, Jesse Young³, Michael R. Fisch⁴, Morgan E. Chaney², Andrew Kramer²,
Metin I. Eren^{2,5}

*Corresponding author: a.j.m.key@kent.ac.uk +44(0)1227 827056

¹ School of Anthropology and Conservation, University of Kent, Canterbury, Kent, CT2 7NR (UK)

² Department of Anthropology, Kent State University, Kent, OH, 44242 (USA)

³ Department of Anatomy and Neurobiology, Northeast Ohio Medical University, Rootstown, OH, 44272 (USA)

⁴ College of Applied Engineering Sustainability and Technology, Kent State University, Kent, OH, 44242 (USA)

⁵ Department of Archaeology, Cleveland Museum of Natural History, Cleveland, OH, 44106 (USA)

35 Abstract

36

37 Diverse disciplines investigate how muscular tissue (i.e. ‘meat’) responds to being cut and
38 deformed, however, large-scale, empirically robust investigations into these matters are often
39 impractical and expensive. Previous research has used clay as an alternative to meat. To
40 establish whether clay is a reliable proxy for meat, we directly compare the two materials via
41 a series of cutting and projectile tests. Results confirm that the two materials display distinct
42 cutting mechanics, resistance to penetration and are not comparable. Under certain conditions
43 clay can be used as an alternative to meat, although distinctions between the two may lead to
44 experimental limitations.

45

46

47

48

49

50

51 Keywords: Force; Fracture; Stone Tool; Material Science; Butchery

52

53

54

55

56

57

58

59

60

61

62

63

64

65

66

67

68

69 1. Introduction

70 A diverse range of disciplines investigate how muscular tissue (i.e. ‘meat’) responds to being
71 cut and deformed under different experimental conditions. Animal products are primarily
72 used in these studies, either as a substitute for human tissue, or when addressing questions
73 relating to the butchery and processing of animal products in ‘real-world’ settings. Of note
74 are ergonomic investigations examining how different cutting tools influence musculoskeletal
75 stresses when processing animal carcasses within industrial settings, engineering and medical
76 research investigating how cutting mechanics and tool use capabilities are influenced by
77 varying cutting edge forms, and archaeological research interested in the relative ability of
78 different artefact types and forms to be used during hunting and butchery activities.

79 The work of McGorry and colleagues are prominent examples from an ergonomic
80 perspective [1]; [2]. In a series of publications examining the implications of blade sharpness,
81 edge angle, and finish on grip forces and moments during modern industrial butchery
82 settings, participants undertook the butchery of beef and lamb in diverse ways (e.g. shoulder
83 boning, intercostal trimming, Y-cutting, shoulder fleecing) and on a relatively large scale (21
84 participants performed the shoulder fleecing and Y-cutting, for example). Szabo et al [3]
85 published similar experiments examining industrial poultry processing. Mechanical and
86 medical engineering research has also examined how aspects of tool-form variation influence
87 their ability to cut biological tissue, but instead often focus on how these variables influence
88 their respective fracture mechanics. Shergold and Fleck [4], for example, used pigskin
89 samples alongside in vivo tests on human skin when examining the relative performance
90 (crack geometry) of sharp and flat-bottomed punches and hypodermic needles. Kasiri et al [5]
91 utilised bovine bones when measuring indentation and failure in cortical bone when cut with
92 a surgical blade. Others have utilised processed meat foodstuffs when investigating the
93 cutting mechanics of associated implements (e.g. wire band saw) in industrial or food
94 preparation settings [6]; [7].

95 Archaeological research has heavily employed experiments that process animal tissues within
96 two research themes. First, numerous publications that have sought to replicate past butchery
97 activities when investigating the relative ability of different tool forms to undertake butchery
98 processes, examinations into the formation of cut marks on bones, and the processes leading
99 to the development of microwear traces (e.g. [8]; [9]; [10]; [11]; [12]; [13]; [14]). Just as
100 prominently, archaeologists have also long been concerned with the projectile technologies of
101 past populations and have frequently undertaken replication experiments investigating form-
102 function relationships and damage formation processes to both tools and targets (e.g. [15];
103 [16]; [17]; [18]). It is notable that Palaeolithic archaeology has a particular emphasis upon
104 such experimentation [19].

105 All fields, however, face issues when using substantial quantities of animal materials in
106 laboratory based experiments. These issues include the expenses of responsibly acquiring and
107 safely disposing of animal tissues; a need for cold storage facilities; relevant health and safety
108 concerns when processing and storing animal products; and the ethical concerns of utilising
109 animal products. While these issues may be somewhat abated in studies of limited scale, they
110 can pose substantial hurdles to large-scale quantitative studies. Further, differences and
111 inconsistencies within animal tissues (muscle fibres, fat, connective tissue etc.) and between
112 carcasses (size, muscle depth, time since death, etc.) may pose problems to studies of cutting
113 mechanics at the micro-scale and comparisons between experimental subjects, respectfully.
114 These concerns have previously been identified by researchers (e.g. [20]) and, at times, led to
115 the use of industrially produced materials as animal product proxies in cutting and projectile
116 experiments. Iovita et al. [21] and Wilkins et al. [22], for example, recently utilised ballistics

117 gelatine instead of animal tissues when examining the functionality of stone tipped weaponry.
118 Similarly, Key, Lycett and colleagues utilised neoprene rubber, polypropylene rope,
119 polythene sheeting, and double-walled corrugated cardboard when testing the relative cutting
120 capabilities of different stone tool forms [23]; [24]; [25]. While such materials may
121 successfully examine the influence of external variables on tool-use capabilities, there are
122 likely key differences in the resistance provided to cutting edges and how fractures initiate in
123 these materials. Certainly, ballistics gelatine has demonstrated differences in the depth of
124 penetration of projectiles and nature of the damage produced when compared to both pig and
125 simulated thoraxes [26]; [27]. Moreover, cardboard and rope display distinct constitutive
126 forms to bio-materials and do not display the typically J-shaped stress-strain curve of meat
127 [28]. So, while such materials are useful and, dependent upon the hypotheses being
128 investigated, are often suitable to be used as a standardised material to be cut, it would be
129 useful to identify an alternative material that negated the above-mentioned problems and
130 displayed similar resistance and fracturing properties to animal tissues.

131 Consequently, past research has both utilised materials that were thought to replicate the
132 cutting mechanics of animal materials, and has directly tested their comparability against
133 animal tissues. McCarthy et al. [29] and Schuldt et al. [7], for example, previously used
134 polyurethane and ethylene propylene diene monomer rubber sheets (respectfully) when
135 examining relationships between sharpness and cutting forces in metallic blades as these
136 materials are considered to display similar fracture mechanics to animal tissues and other
137 similar bio-materials. Marsot et al. [30], on the other hand, compared the shear strength of
138 meat against a series of synthetic materials, and identified a relatively dense polyolefin-based
139 foam as displaying both similar shear strength and cutting forces to meat. Shergold and Fleck
140 [4: 841] went into much greater detail when outlining why silicone rubber may be considered
141 as an “approximate substitute for human skin”, providing a detailed review of the mechanical
142 properties of both materials when being cut. Kalcioglu et al. [31] similarly examined the
143 mechanical behaviours of animal tissues and industrially produced materials, but in this
144 instance compared the penetrability, energy dissipation, and deformation mechanics of heart
145 and liver tissues against a series of tissue simulant gels in projectile tests. Their results
146 indicated that even the best simulant gel still exceeded the penetration depths of the animal
147 tissues by at least ~15%.

148 As suggested by McGorry et al. [20]; [32], clay may also provide a suitable alternative to
149 animal tissues during cutting experiments. In a study examining how task station and blade
150 orientation variation influences gripping forces, cutting moments, and upper limb kinematics
151 during a cutting task using a knife, they suggested that modelling clay provided cutting
152 moments similar to “sirloin and London broil cuts of beef” [20: 1644]. Others have utilised
153 clay during controlled ballistics and cutting experiments when recording penetration levels
154 when protected by different body armour fabrics [33] and deformation and failure rates in
155 clay substrate when cut with tines [34] (although neither used clay as a direct proxy for
156 biological tissues). While clay may intuitively appear similar meat in several important ways
157 (e.g. resistance to a cutting edge), they represent two materials with very distinct
158 compositions, with meat being a fibrous organic tissue and clay primarily being formed of
159 silicate particles and trapped water. Moreover, there has yet to be a controlled experimental
160 investigation specifically addressing the relative ability of clay to provide an accurate
161 alternative to meat.

162 Here we redress this issue and assess the suitability of fresh potters clay to be used as an
163 alternative to meat during cutting and projectile activities. Specifically, we undertake two
164 rounds of experiments. The first examines the forces and deformation required to cut clay and

165 meat of equal measure with a straight, homogeneous metallic blade. The second examines the
166 ability of modern metallic composite arrows and Palaeolithic stone projectiles to penetrate
167 clay and meat when fired at a controlled speed and distance. We conclude by discussing the
168 nature of any similarities or differences in the two materials and the suitability of using clay
169 as a substitute to meat in future archaeological, ergonomic, and engineering experiments.

170

171 **2. Loading Rates during Cutting**

172 The relative ability of sharp edged tools to initiate fractures in materials and permanently
173 separate two or more of their aspects is of broad importance to many areas of research (see
174 Atkins [2009] and examples therein). Consequently, examinations into the forces required to
175 cut materials with metal knives, stone tools, and other implements have taken many forms,
176 including the use of pressure sensitive pads attached to the hands, force sensors beneath
177 worked materials, and finite element modelling (e.g. [1]; [35]; [36]). Here we use an
178 approach widely used within fracture mechanics research [7]; [29]; [37].

179 Forces and deformation levels during cutting were recorded here using an Instron® 5500
180 universal tensile testing system (Fig. 1). We used 30 steel 2-facet utility (razor) blades
181 (Kolbalt®) during the cutting tests, all of which were secured into 70x38x18 mm wooden
182 blocks. Each blade was fixed into a block such that only 24mm of cutting edge remained
183 exposed (Fig. 1). The blocks were secured into the upper grip of the testing machine and each
184 blade was used to cut both materials (Fig. 1). The clay was low-fire potters clay bought from
185 Standard Ceramic Supply Company (Pittsburgh, USA) and the meat (beef) was chosen to
186 contain limited intramuscular fat or connective tissue. Tissue fibre direction was not
187 controlled in the meat. All blades cut the clay first and then the meat. 20 mm thick portions of
188 each material were placed on a secure wooden platform beneath the grip (the latter material
189 required additional securing with coarse sandpaper at its base to prevent movement during
190 cutting). There was slight variation in the thickness of the meat due to it deforming and
191 flexing when being cut into portions. The wooden platform was aligned so that only 20 mm
192 of each material was beneath the blade's exposed edge. Beneath the portion of material being
193 cut there was a 5mm gap in the wooden platform, into which the blade entered as it cut
194 through the material.

195 The crosshead, into which the grip and blades were fixed, was lowered prior to the test so that
196 the tip of the blade's edge was in contact with the material surface (but applying no pressure).
197 At this point the displacement reading was set to zero. The blades were lowered into each
198 material at a rate of 20 mm/min. Displacement (mm) and force (N) levels were recorded for
199 each controlled cut, which continued until the blade passed through the material in its
200 entirety. Two sampling frequencies were used in each test. The first 7mm of deformation was
201 recorded at a rate of 10 Hz, after which the sampling frequency dropped to 2 Hz. This
202 allowed a greater level of detail to be recorded at the point of cut initiation and/or initial
203 material deformation.

204

205 **3. Penetrability during Projectile Use**

206 The aim of our second test was to investigate the resistance provided by clay and meat targets
207 when struck by projectile points. We investigated this by comparing the depth of penetration
208 achieved by modern metal composite arrows and Palaeolithic replica stone points when fired
209 from a standardised distance, angle, and speed. If each material returned similar penetration

210 distances and levels of variation, then it may be suggested that clay could be a suitable
211 alternative to meat within studies of projectile weaponry. Penetration depths were recorded
212 from 204 composite arrow shots, being fired into the clay and meat 102 times each. Similarly,
213 penetration depths were recorded from 60 replica stone point shots, striking the meat and clay
214 30 times each. Following this, we used high-speed video to analyse three-dimensional (3D)
215 projectile impact dynamics (i.e., ballistics) of an additional 19 shots fired into meat and 18
216 shots fired into clay.

217 The clay target was formed of 45.4 kg of material and was shaped into an orthorhombic
218 cuboid measuring 22x25x45 cm³ (Fig. 2). As in the cutting experiment, the clay was low-fire
219 potter's clay bought from Standard Ceramic Supply Company (Pittsburgh, USA). In all
220 instances during shaping the clay was compressed (wedged) to ensure no pockets of air were
221 present. Due to the differential size of the projectiles, this was repeated after every 20 shots
222 for the arrows and every 10 shots for the stone points. The meat target was formed from 12.7
223 kg of beef rump that did not contain any bone or skin. Intramuscular fat and connective tissue
224 was, again, minimal. Six 'rump roasts' were lined up to form a target 45 cm deep, before
225 being surrounded on five sides by a ~5 cm clay wrap (Figs. 2E and 2F). The clay 'wrap' was
226 pulled taught, such that it enveloped the beef and provided resistance to its edges. The beef
227 was replaced every 30 shots for the arrows and every 5 shots for the stone points. Both
228 materials were supported on a wooden platform 1 m from the floor and 3.5 m from the tip of
229 the projectiles at the point of release (Fig. 2). At the point of release the projectiles were 125
230 cm from the ground and, therefore, aligned with the top of the clay target. Projectiles were,
231 however, aimed at the centre of the clay, meaning that there was a very slight slope at the
232 point of entry. Data was only collected from the clay when the projectiles entered more than
233 5 cm from its edge (Fig. 2D). Due to the clay surrounding the meat, all shots that were on
234 target for this material were counted, so long as no clay was struck. Data were only ever
235 collected from projectiles that impacted on portions of material that maintained surface
236 integrity and had not been hit by previous shots.

237 75 cm long Easton (XX75 Tribute 1616) metal alloy arrows weighing 20.6 g and with
238 diameter of 6 mm were used as the composite arrow (Fig. 3). The stone tipped projectiles
239 (Fig 3) were lanceolate points made from Texas chert (Fredericksburg variety), produced by
240 C. Ratzat (www.neolithics.com). All stone points used were similar in morphology, having
241 been ground into the following form using modern lapidary equipment: 76.2 mm length;
242 27.94 mm medial width; and 7.94 mm medial thickness, with the thickness tapering toward
243 the point's tip, base, and lateral edges. The stone points were then hafted by R. Berg
244 (www.thunderbirdatlatl.com) on one-meter long shafts of air-dried ash wood, which is
245 extremely resilient and resistant to bending and breakage (Berg, personal communication).
246 The diameter of each shaft was approximately 10.25 mm. The adhesive used for the hafting
247 was heated bone glue, which was specifically developed by Berg. The material used for the
248 lashings was an animal-based silk fibre from bovines.

249 Both the arrows and the stone tipped projectiles were fired from a 29 lbs compound
250 bow fixed to an automatic compound bow stand (Spot-Hogg 'Hooter Shooter'), allowing for
251 precision shooting at predefined draw lengths and velocities. All arrows were fired at a target
252 speed of 30.5 meters per second (m/s), whereas the stone points were fired at a target speed
253 of 25 m/s. Limited variation was to be expected in each case due to the ratcheting system
254 used to draw the bow, minute differences in arrow notch contact with the drawstring, and
255 negligible deviations in projectile trajectory. All projectiles were fired through a Shooting
256 Chrony chronograph, allowing their precise speed to be recorded as it passed through the two
257 aspects of its triangular frame, activating photo-resistors set at a known distance from one

258 another. Depth of penetration was recorded for both projectile types in millimetres (mm) and
259 was measured from the tip of the arrow's point to the first aspect of the shaft that remained
260 outside of the target material.

261 We used two synchronised high-speed cameras (Fastec HiSpec Lite cameras, Fastec Imaging,
262 San Diego, CA USA) to quantify the dynamics of how each projectile impacted the two
263 different materials. The cameras were operated at a frame rate of 800 Hz, shuttered at a rate
264 of 8000 Hz (i.e., exposure duration of 0.125 ms) to minimise motion blur, and synchronised
265 by means of a common push button trigger. Prior to each experiment, we affixed a series of
266 six bands of retro-reflective tape (Scotchlite Brand, 3M Corporation, St. Paul, MN USA)
267 along the shaft of each arrow to provide high-contrast features for subsequent digitising of
268 projectile motion (Fig. 2F). We calibrated the two-dimensional images from each camera to a
269 common 3D coordinate frame following the methods of Theriault et al [38], using their freely
270 available "easyWand" toolbox for MATLAB (MathWorks Inc., Natick, MA USA). Briefly,
271 we calibrated a volume approximately 1 m by 1 m by 0.5 m immediately surrounding the
272 projectile target using the Sparse Bundle Adjustment (SBA) algorithms in the easyWand
273 toolbox. The program takes as input the digitised x,y pixel position of "background" points
274 visible to both cameras (i.e., any discrete feature identifiable in the volume of interest). An
275 object of known length – the "wand" – is also filmed moving through the volume to
276 transform image dimensions into real-world units (i.e., meters) and to provide additional
277 reference features for the SBA calibration. The SBA algorithm combines the apparent planar
278 position of all of these features with data on intrinsic parameters of the cameras (e.g., lens
279 focal length, radial distortion properties of the lenses, camera sensor size, and principal focal
280 point on the sensor) to generate a set of Direct Linear Transformation (DLT) coefficients that
281 precisely describe the position of each camera in space [39]. Using these calibrations, we
282 were able to localise the 3D position of moving projectiles with an accuracy of 1.75-2.5 mm.
283 Finally, we entered the DLT coefficients into the DLTdv5 motion-tracking toolbox for
284 MATLAB [40], and used this software to digitise the 3D x,y,z position of the reflective
285 markers spaced along each projectile's shaft during the period of impact.

286

287 **4. Data Analysis**

288 4.1 Cutting

289 Loading (N) and blade displacement (mm) were recorded during each cutting test. In turn, it
290 was possible to visualise load-displacement curves during each cut and material stiffness
291 (calculated from the slope between adjacent data points after smoothing [N/mm]) relative to
292 blade displacement. Shapiro-Wilk tests confirmed that although the maximum loading levels
293 for both materials and the mean loading levels for the clay were normally distributed ($p =$
294 $.162-.803$), the mean loading levels required to cut the meat were not ($p = .005$). Hence,
295 Mann-Whitney U tests ($\alpha = .05$) were used to statistically compare the maximum and mean
296 loads recorded in the cutting tests of the two materials. Maximum loads were defined as the
297 greatest load recorded at any point during the cutting test. Mean loads were calculated from
298 the point at which data collection started up until the blade had fully emerged through the
299 portion of material (i.e. displacement = 39 mm). Only one in every five data points for the
300 first 7mm of cutting was utilised for the calculation of mean load (so that all data in this
301 measure was equivalent to a sampling rate of 2 Hz). Differences in the load-displacement
302 curves and stiffness plots of the two materials are also compared.

303

304 4.2. Projectiles

305 Projectile speed and depth of material penetration was recorded for both the metal arrows (n
306 = 102) and stone points (n = 30) in each of the two materials. Shapiro-Wilk tests identified
307 the penetration depths of both projectiles during the meat test to be normally distributed (p =
308 .498 and .766 for the arrow and stone point, respectively). Whereas the stone point clay data
309 was normally distributed (p = .610), the penetration depths returned for the arrow when fired
310 into the clay was not (p = .010). Hence, we used non-parametric aligned rank-transformed
311 analyses of variance (ANOVAs) to analyse these data [41]. Aligned rank-transformed
312 ANOVA is a non-parametric alternative to a standard parametric two-way ANOVA that
313 permits testing of both main effects and interactions in a full-factorial design. In the case of
314 significant interactions, Mann-Whitney U tests were used for post-hoc analyses of within cell
315 differences (i.e., differences between responses to different material types within a given
316 projectile type). P-values for post-hoc tests were adjusted using the False Discovery Rate
317 procedure [42] to control for experiment-wise Type I error inflation.

318 The dynamics of projectile impacts (i.e., impact ballistics) were analysed from motion-
319 tracked video data using a custom-written MATLAB program. We first fit raw x, y, z
320 coordinate data to a quintic smoothing spline (i.e., MATLAB's SPAPS function, set to a
321 tolerance of 10^{-5} mm²), providing a parameterised function describing instantaneous projectile
322 displacement with respect to time. Instantaneous projectile velocity was subsequently
323 calculated as the first derivative of the smoothing spline. Instantaneous fore-aft (i.e., X),
324 mediolateral (i.e., Y), and vertical (i.e., Z) axis displacement and velocity vectors were then
325 resolved into two planar components – one acting along the projectile's principal trajectory
326 (i.e., axial displacement and velocity), and a second acting normal to this trajectory (i.e.,
327 tangential displacement/velocity). Impacts were characterised by a rapid drop in axial
328 velocity, during which the projectile decelerated from launching velocity to zero over a
329 period of milliseconds (Fig. 4). We operationally defined the period of impact as beginning
330 with the first frame in which axial velocity dropped below baseline launching speed, and
331 ending when axial velocity reached zero. We then calculated several variables characterising
332 the dynamics of the projectile's interaction with the target material during impact (Table 1).

333 We analysed a total of 37 high-speed video trials, including 19 trials with composite arrows
334 (9 in clay and 10 in meat) and 18 trials with stone points (9 each in clay and meat). Given the
335 relatively small sample sizes for each of the four experimental conditions, and the non-
336 normality of several subsamples for particular experimental conditions, we used non-
337 parametric aligned rank-transformed analyses of variance (ANOVAs) to analyse these data.
338 In the case of significant interactions, Mann-Whitney U tests were used for post-hoc analyses
339 of within cell differences (i.e., differences between responses to different material types
340 within a given projectile type), adjusting p-values using the False Discovery Rate procedure
341 [42]. All statistical procedures were implemented in the R statistical package (R Core Team,
342 2017), supplemented by the ARTool add-on package [41].

343

344 5. Results

345 5.1 Cutting

346 Each cutting test produced 400-500 data points for both load (N) and displacement (mm).
347 There are clear differences in the loading levels required to cut the two materials with mean
348 loads being roughly twice as great during the meat test relative to the clay, whereas maximum
349 loads were nearly three times as great (Table 2). Mann-Whitney U tests confirmed that

350 maximum and mean loading levels were significantly different between the two materials (p
351 = .0001 in each instance). There are also differences between the two materials in terms of
352 the variation observed in loading as the meat's coefficient of variation levels are more than
353 double that of the clay (Table 2). Levene's test for homogeneity of variance returned
354 significant results between each material for both mean and maximum values (p = .0001 and
355 .0002, respectfully).

356 Figure 5 details typical load-displacement curves and material stiffness plots for each of the
357 cut materials. As expected, the meat displays a J-shaped curve such that as the cutting edge
358 starts to move towards the tissue (i.e. low displacement) it deforms under relatively low loads
359 without fracturing. At larger displacement levels the meat stiffens and provides increasing
360 resistance to the blades edge until such a point that any increased extension creates stress
361 enough to permanently fracture the muscle fibres (i.e. a cut is formed). As detailed in Figure
362 5B, this process of load increases and then groups of muscle fibres fracturing repeats until the
363 blade has passed through all of the muscle tissue. The stiffness plots for the meat follow the
364 load-displacement curves and highlight both the 'bunching' nature of the muscle fibres and
365 how stiffness increases when the meat is under relatively high deformation (Fig. 5D).

366 The clay displays a load-displacement curve that is highly consistent between samples (Fig.
367 5A) and similar to those returned by Wang and Gee-Clough [34]. There were no obvious
368 points at which fractures were initiated in the material and the greatest stiffness was recorded
369 for the first ~3 mm when the blade first entered the clay block. Stiffness also marginally
370 increased towards the end of the cutting events when the greatest amount of the blade's
371 surface area was in contact with the clay. Peak stiffness levels were substantially lower
372 within the clay condition relative to the meat. Loading levels increase sharply at first and then
373 more steadily until displacement reaches ~20 mm, before exhibiting a reverse trend of
374 decreasing relatively sharply and then levelling out. Peak loading is consistently at the point
375 prior to the blade's edge cutting through the bottom of the 20mm of clay. Consequently, it
376 appears that the meat and clay display very different fracture mechanics, and that the clay
377 displays very low elastic deformation prior to fracturing.

378

379 5.2 Projectiles

380 5.2.1 Penetration depth and speed

381 Descriptive statistics for the penetration depths and speeds of each projectile and material
382 type are presented in Table 3. It is clear that both the composite arrows and stone points
383 display differences in penetration depths when fired in the meat and clay, with the meat
384 appearing to be more resistant (Fig. 6). Aligned rank-transformed ANOVA indicates the main
385 effects for both projectile type and material type, and a significant projectile-by-material type
386 interaction (Table 4). Specifically, the relative differences achieved by the stone points
387 between the clay and meat is substantially lower than that observed for the arrows. Indeed, on
388 average, arrows achieved penetration depths in clay that are roughly twice that of meat (Table
389 3; Fig. 6). As expected, given the systematic method for launching the projectiles, speed did
390 not vary between the target material types, and there was no significant interaction between
391 projectile type and material type. However, the lighter composite arrows were launched at
392 significantly greater speeds than the relatively heavy stone points (Tables 3 and 4; Fig. 6).

393 5.2.2 High-speed video analyses of projectile impact dynamics

394 5.2.2.1 Validation

395 Summary statistics from the high-speed dataset are presented in Table 5. We used two
396 methods to assess the validity of high-speed video based measures of projectile impact
397 dynamics, relative to the other objective methods discussed above. First, we compared peak
398 axial speed of the projectiles in our motion-tracking dataset to the launching speeds measured
399 in the more extensive chronograph dataset. Peak axial speeds of composite arrows were
400 slightly higher than the speeds in the chronographic dataset, with an average of 34.4 m/s
401 (bootstrapped 95% CI: 33.7 - 35.1 m/s) (Table 5), whereas peak axial speeds for the stone
402 points were slightly lower, with an average of 23.4 m/s (bootstrapped 95% CI: 22.5 - 24.3
403 m/s). Overall, the speeds measured by the two methods were similar, with some variation
404 expected due to random variation among experimental days and measuring speeds at slightly
405 different locations (i.e., chronograph speeds were measured immediately after launching,
406 whereas motion-tracking data were taken closer to the impact with the target).

407 Second, we also assessed validity of our high-speed video dataset by directly comparing
408 impact displacement estimated from motion-tracking to direct measurements of penetration
409 depth from the projectile embedded in the target (note that direct measurements of
410 penetration depth were only available for a subset of 23 trials). Although these two
411 measurements are not expected to be identical, given that there could be residual movement
412 and recoil of the projectile after the initial impact, the two measures should be close to one
413 another. Overall, impact displacement and penetration depth were highly correlated (Fig. 7;
414 Pearson's $r = .960$, $p < .001$). A least-squares linear regression fit indicated that measured
415 depth scaled to estimated depth with a slope of 1.08 (95% CI: 0.936 - 1.22 and a y-intercept
416 of -21.5 mm (95% CI: -44.5 - 1.59 mm). These scaling values are not significantly different
417 from a line of identity (i.e., slope of 1.0 and intercept of 0) (Fig. 7). Moreover, residual
418 deviations between estimated and measured penetration depths were not significantly
419 positively nor negatively biased relative to zero (Fig. 7; binomial test: $p = .210$).

420 5.2.2.2 Impact Dynamics

421 The results of the two-way aligned rank-transformed ANOVAs of impact dynamics are
422 summarised in Table 6. Variation in impact displacement was characterised by significant
423 main effects for both projectile type and material type, and a significant projectile by material
424 interaction (Table 6). Post-hoc tests revealed that for composite arrows, shots into a clay
425 target were characterised by greater impact displacement than shots into meat targets. Stone
426 points, by contrast, showed no significant variation in impact displacement between the two
427 materials (Fig. 8a). Similar results were obtained in the larger penetration depth dataset
428 discussed above, where we found that material-based differences in penetration depth were
429 attenuated for stone points versus composite arrows. Variation in impact duration was
430 characterised by a significant main effect for material type, and a significant projectile by
431 material interaction, but not a significant main effect for projectile type alone. Post-hoc tests
432 revealed that material type had opposite effects between the two projectile types, with clay
433 targets being characterised by significantly longer impact durations for composite arrow
434 shots, but meat targets being characterised by significantly longer impact durations for stone
435 point shots (Fig. 8b). Work of impact did not vary between materials or show a significant
436 projectile by material type interaction, only showing a significant main effect for projectile
437 type, with shots by stone points being characterised by significantly greater work of impact
438 than composite arrow shots (Fig 8c). Finally, variation in average impact force was
439 characterised by a significant main effect for projectile type and a significant projectile by

440 material interaction, though the main effect for material type was not significant. Post-hoc
441 analyses showed that average impact force was significantly greater for meat targets for shots
442 by composite arrows, whereas average impacts forces were similar across material types for
443 shots by stone points (Fig. 8d).

444

445 **6. Discussion and Conclusion**

446 The use of industrially produced and/or synthetic materials as a substitute for ‘meat’ is
447 common within a diverse range of disciplines. This includes the use of fresh clay, which has
448 been suggested to be a suitable alternative to the use of meat during examinations of the
449 ergonomic consequences of using different hand-held cutting tools [20]; [32]. Here we
450 present a series of experiments that directly test whether clay is a reliable proxy for meat
451 during cutting and projectile research.

452 Results indicate that when similarly sized portions of clay and meat are cut, the maximal and
453 mean forces required to cut through meat are significantly greater than those required for
454 clay. Indeed, mean force requirements for meat are roughly twice that of clay, while
455 differences in maximum forces are three times as great. In short, meat provides greater
456 resistance to a cutting edge than clay. Although we can only speak of the extent of this
457 difference for beef, we believe it is reasonable to assume that other meats will display similar
458 results. The greater difference recorded for the maximum force records appear to have been
459 caused by both the presence of sinuous connective tissue in the meat and muscle fibres
460 ‘bunching up’ to provide greater resistance to blade cutting edges. Certainly, although care
461 was taken to avoid connective tissue in all meat portions, trials 19, 20, and 24 appeared near
462 absent of this material and, in turn, returned some of the lowest maximal force records.
463 Inconsistencies in the material structure of meat also likely contributed to the greater
464 coefficient of variation levels returned for this material, which are double that of clay.

465 Differences between the materials are highlighted by the load-displacement curves that detail
466 how each material propagates fractures (i.e. cuts). Clay is characterised by very consistent
467 curves between individual tests that are, at least partially, representative of the amount of
468 surface area of blade wedged between the clay at a given time (i.e. the amount of blade
469 surface area that could possibly make contact with the clay, both at the blade’s edge and
470 sides). Certainly, it is clear that as the blade starts to exit the clay and no more material is
471 being cut, force reduces in a consistent manner. Further, the greatest force is recorded at a
472 blade displacement of 20 mm, when the entirety of the blade’s surface area is within the clay
473 (Fig. 5). In other words, some of the resistance provided by the clay appears to be caused by
474 friction acting against the surface of the blade. It is, however, clear that the first ~2.5 mm of
475 displacement (i.e. when the blade’s tip enters the clay) displays a notable increase in force
476 relative to displacement (Fig. 5). This is consistent between individual clay tests. The clay
477 was fresh in all instances, so we do not think this trend can be attributed to a ‘skin’ forming
478 on the outside of the material samples. Blade tip geometry appears to be the cause of this
479 phenomenon as the wedged aspect was 2 mm deep, meaning that resistance progressively
480 increased for the first 2 mm of displacement. As highlighted by Wang and Gee-Clough [34]
481 there was likely a combination of wedge and sheer distortion dependent on the
482 micromorphology of the blades tip, however, in contrast to their study and in line with
483 Stafford [43], fracture propagation is likely to be best described as a flow pattern and not
484 material failure.

485 Conversely, meat displays a J-shaped curve where it initially easily deforms without
486 fracturing, but goes on to stiffen, provide increases resistance to the cutting edge, and then

487 finally fractures when extension and loading creates enough stress in the material. In this way
488 meat builds up tension and resistance to fracture as muscle fibres ‘bunch-up’ before
489 fracturing, in turn leading to the characteristic ‘jagged’ load-displacement curve as the blade
490 cuts through the meat (Figure 5). In contrast, the clay displays no obvious points at which
491 fractures occur. Further, meat undergoes elastic deformation prior to fractures initiating, such
492 that edge loading does not, at least at the very start of cutting processes, create irreversible
493 damage to the material’s surface. Clay, however, at first displays minimal plastic deformation
494 before parting and forming material separation. It is unclear whether at a microscopic level
495 clay displays elastic deformation. It is important to highlight that the addition of variation in
496 rake angle, direction of cutting, included (edge) angle, cutting edge size and surface area, and
497 slice-push ratio may alter the strength of relationship observed here, but are unlikely to
498 change the overall distinction in material performance.

499 Meat and clay do, therefore, display clear differences in their fundamental cutting mechanics.
500 This is not particularly surprising and, in turn, clay would not make a suitable alternative to
501 meat during tests of cutting edge fracture mechanics during meat processing behaviours. The
502 results presented here also clearly detail that there are significant differences in the resistance
503 provided to cutting edges between these two materials. However, experiments concerned
504 with the consequences of meat cutting, such muscle fatigue during tool use or torque
505 experienced by a hand-held tool, may reasonably use clay as a replacement for meat, so long
506 as they are aware of the differences in required forces. McGorry [20]; [32] was, therefore,
507 justified in his use of clay as a substitute for meat when examining gripping forces and upper
508 limb kinematics during knife use, although the present results suggest that the forces recorded
509 in these experiments may be less than those experienced in ‘real-world’ butchery events.
510 Future experiments may profitably examine whether other meats, such as poultry, return
511 similar results to those provided here, and how different types of clay (e.g. modelling or
512 kaolin) compare to the potters’ clay used here.

513 The projectile tests returned similar results to the cutting tests insofar as meat provided
514 greater resistance to penetration than clay. It is notable, however, that relative differences
515 between the two materials for the stone points is substantially lower than it is for the
516 composite arrows. That is, in terms of depth of penetration, clay appears a closer proxy for
517 meat for stone points than for the composite arrows. These results are corroborated by the
518 high-speed video analyses of each projectile’s impact dynamics when fired into the two
519 materials: clay provided significantly greater impact displacement than the meat for the
520 composite arrows, but no significant difference for the stone points. Therefore, even though
521 the work of impact is similar (because the loss of kinetic energy is similar, given that the
522 arrows were travelling at set speeds), the average force required to stop the arrow is greater
523 for shots into meat. The differences in the comparability of clay and meat, dependent on the
524 projectile, is likely due to the form and mass of each projectile. That is, despite the stone
525 point displaying greater work of impact, its greater surface area meant that its energy
526 dissipated in totality at earlier depths of penetration. In turn, there was reduced potential for
527 any disparities between meat and clay to accrue into significant differences. In sum, the high-
528 speed video analyses and depth of penetration tests suggest that, dynamically, clay can be
529 used as a suitable substitute for meat during experimental archaeology tests with stone points,
530 but not for modern composite arrows. That is, for studies concerned with the performance of
531 reasonably large projectile tips (such as those often observed in the Palaeolithic
532 archaeological record), clay may be used as reliable proxy for meat. In sum, when both sets
533 of tests are combined, it appears that clay has the potential to be of use within cutting and
534 projectile experiments, however, caution should be used when assessing its suitability as a
535 reliable proxy for meat.

536

537 **Acknowledgements**

538 AK's research is supported by a British Academy Postdoctoral Fellowship (pf160022). We
539 thank J. Valli for assistance with high-speed video analysis. MIE is supported by the Kent
540 State University College of Arts and Sciences and by the National Science Foundation (NSF
541 Award ID: 1649395). We are grateful for the anonymous reviewer's constructive criticism
542 and detailed comments, and for the assistance of the editorial team.

543

544

545

546 **References**

- 547 [1] McGorry R.W., Dowd P.C. and Dempsey P.G. 2003. Cutting moments and grip
548 forces in meat cutting operations and the effect of knife sharpness. *Applied*
549 *Ergonomics* 34: 375-382
- 550 [2] McGorry R.W., Dowd P.C. and Dempsey P.G. 2005. The effect of blade finish and
551 blade edge angle on forces used in meat cutting operations. *Applied Ergonomics* 36:
552 71-77
- 553 [3] Szabo R.L., Radwin R.G. and Henderson C.J. 2001. The influence of knife dullness
554 on poultry processing operator exertions and the effectiveness of periodic knife
555 steeling. *American Industrial Hygiene Association Journal* 62(4): 428-433
- 556 [4] Shergold O.A. and Fleck N.A. 2005. Experimental investigation into the deep
557 penetration of soft-solids by sharp and blunt punches, with application to the piercing
558 of skin. *Journal of Biomechanical Engineering*, 127(5): 838-848
- 559 [5] Kasiri S., Reilly G. and Taylor D. 2010. Wedge indentation fracture of cortical bone:
560 experimental data and predictions. *Journal of Biomechanical Engineering* 132 (8):
561 081009
- 562 [6] Atkins, A.G., Xu X. and Jeronimidis G. 2004. Cutting, by 'pressing and slicing,' of
563 thin floppy slices of materials illustrated by experiments on cheddar cheese and
564 salami. *Journal of Materials Science* 39: 2761-2766
- 565 [7] Schuldt S., Arnold G., Kowalewshi J., Schneider Y. and Rohm H. 2016. Analysis of
566 the sharpness of blades for food cutting. *Journal of Food Engineering* 188: 13-20
- 567 [8] Keeley, L.H. 1980. *Experimental Determination of Stone Tool Uses: a Microwear*
568 *Analysis*. The University of Chicago Press, Chicago
- 569 [9] Jones P. 1980. Experimental butchery with modern stone tools and its relevance for
570 Palaeolithic archaeology. *World Archaeology* 12 (2): 153-165
- 571 [10] Willis L., Rick T., Eren M.I. 2008. Does butchering fish leave cutmarks?
572 *Journal of Archaeological Science* 35:1438-1444.
- 573 [11] Bello, S.M., Parfitt S.A. and Stringer C., 2009. Quantitative
574 micromorphological analyses of cut marks produced by ancient and modern
575 handaxes. *Journal of Archaeological Science* 36 (9): 1869-1880
- 576 [12] Merritt S.R. 2012. Factors affecting Early Stone Age cut mark cross-sectional
577 size: implications from actualistic butchery trials. *Journal of Archaeological Science*
578 39(9): 2984-2994
- 579 [13] Braun D.R., Pante, M., and Archer W. 2016. Cut marks on bone surfaces:
580 influences on variation in the form of traces of ancient behaviour. *Interface Focus*
581 6(3): 20160006

- 582 [14] Gingerich J.A.M. and Stanford D.J. in press. Lessons from Ginsberg: An
583 analysis of elephant butchery tools. *Quaternary International*
584 doi:10.1016/j.quaint.2016.03.025
- 585 [15] Smith M.J., Brickley M.B., and Leach S.L. 2007. Experimental evidence for
586 lithic projectile injuries: improving identification of an under-recognised
587 phenomenon. *Journal of Archaeological Science*, 34(4): 540-553
- 588 [16] Churchill S.E., Franciscus R.G., McKean-Peraza H.A., Daniel J.A., and
589 Warren B.R. 2009. Shanidar 3 Neandertal rib puncture wound and paleolithic
590 weaponry. *Journal of Human Evolution*, 57(2): 163-178
- 591 [17] Sisk M.L. and Shea J.J. 2009. Experimental use and quantitative performance
592 analysis of triangular flakes (Levallois points) used as arrowheads. *Journal of*
593 *Archaeological Science* 36 (9): 2039-2047
- 594 [18] Pargeter J., Shea J., and Utting B. 2016. Quartz backed tools as arrowheads
595 and hand-cast spearheads: Hunting experiments and macro-fracture analysis. *Journal*
596 *of Archaeological Science* 73: 145-157
- 597 [19] Eren M. I., Lycett S. J., Patten R.J., Buchanan B, Pargeter J., O'Brien, M. J.
598 2016. Test, model, and method validation: the role of experimental stone artifact
599 replication in hypothesis-driven archaeology. *Ethnoarchaeology* 8:103-136
- 600 [20] McGorry R., Dempsey P.G. and O'Brein N. 2004. The effect of work station
601 and task variables on forces applied during simulated meat cutting. *Ergonomics*
602 47(15): 1640-1656
- 603 [21] Iovita R., Schönekeß H., Gaudzinski-Windheuser, S., and Frank Jäger. 2014.
604 Projectile impact fractures and launching mechanisms: results of a controlled ballistic
605 experiment using replica Levallois points. *Journal of Archaeological Science*, 48: 73-
606 83
- 607 [22] Wilkins J., Schoville B.J., and Brown K.S. 2014. An experimental
608 investigation of the functional hypothesis and evolutionary advantage of stone-tipped
609 spears. *PLoS One*, 9(8): e104514
- 610 [23] Key, A.J.M. and Lycett, S.J. 2011. Technology based evolution? A biometric
611 test of the effects of handsize versus tool form on efficiency in an experimental
612 cutting task. *Journal of Archaeological Science* 38 (7): 1663-1670
- 613 [24] Key, A.J.M., Proffitt, T., Stefani, E., and Lycett S.J. 2016. Looking at
614 handaxes from another angle: Assessing the ergonomic and functional importance of
615 edge form in Acheulean bifaces. *Journal of Anthropological Archaeology* 44(A): 43-
616 55
- 617 [25] Key, A.J.M. and Lycett, S.J. 2017. Reassessing the production of handaxes
618 versus flakes from a functional perspective. *Archaeological and Anthropological*
619 *Sciences* 9 (5): 737-753
- 620 [26] Karger B., Sudhues H., Kneubuehl B.P., and Brinkman B. 1998. Experimental
621 arrow wounds: ballistics and traumatology. *Journal of Trauma and Acute Care*
622 *Surgery*, 45(3): 495-501.
- 623 [27] Mabbott A., Carr D.J., Champion S., Malbon C. 2016. Comparison of porcine
624 thorax to gelatine blocks for wound ballistics studies. *International Journal of Legal*
625 *Medicine*, 130(5): 1353-1361
- 626 [28] Atkins, T. 2009. *The Science and Engineering of Cutting: The Mechanics and*
627 *Processes of Separating, Scratching and Puncturing Biomaterials, Metals and Non-*
628 *Metals*. Butterworth-Heinemann, London
- 629 [29] McCarthy C.T., Hussey M. and Gilchrist M.D. 2007. On the sharpness of
630 straight edge blades in cutting soft solids: Part I – indentation experiments.
631 *Engineering Fracture Mechanics* 74: 2205-2224

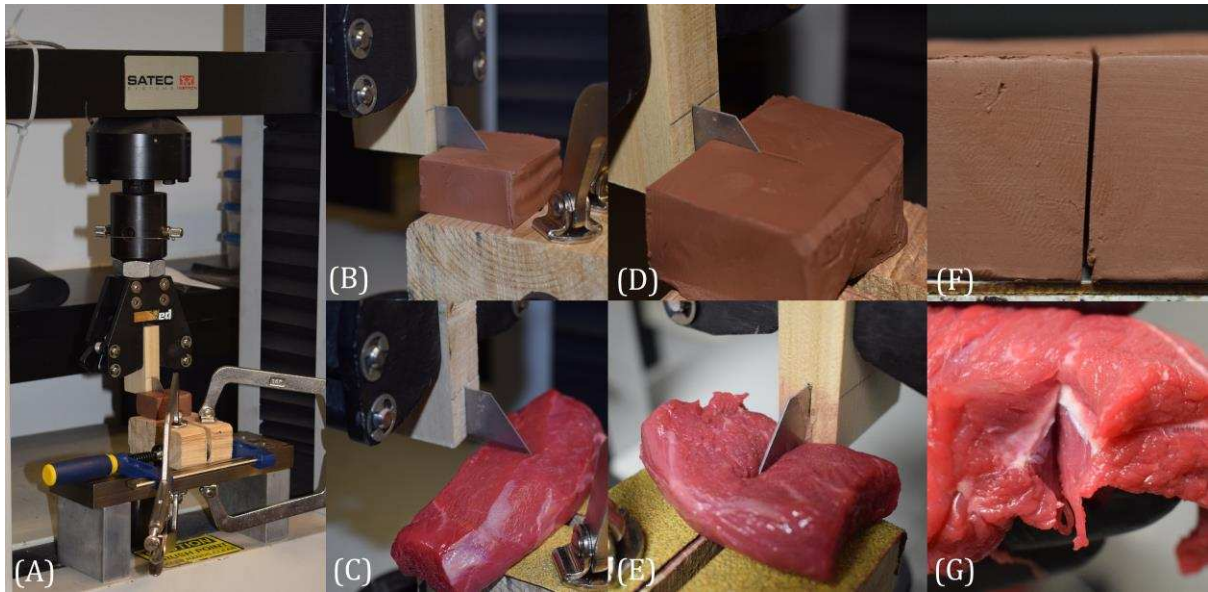
- 632 [30] Marsot J., Claudon L., and Jacqmin M. 2007. Assessment of knife sharpness
633 by means of a cutting force measuring system. *Applied Ergonomics*, 38(1): 83-89
- 634 [31] Kalcioglu Z.I., Qu M., Strawhecker K.E. Shazly T., Edelman E.,
635 VanLandingham M.R., Smith J.F., and Van Vliet K.J. 2011. Dynamic impact
636 indentation of hydrated biological tissues and tissue surrogate gels. *Philosophical*
637 *Magazine* 91(7-9): 1339-1355
- 638 [32] McGorry R.W. 2001. A system for the measurement of grip forces and applied
639 moments during hand tool use. *Applied Ergonomics* 32: 271-279
- 640 [33] Lee B.-W., Kim I.-J., and Kim C.-G. 2009. The influence of the particle size
641 of silica on the ballistic performance of fabrics impregnated with silica colloidal
642 suspension. *Journal of Composite Materials*, 43(23): 2679-2698
- 643 [34] Wang J. and Gee-Clough D. 1993. Deformation and failure in wet clay soil:
644 part 2, soil bin experiments. *Journal of Agricultural Engineering Research*, 54(1): 57-
645 66
- 646 [35] Arcona C. and Dow T.A. 1996. The role of knife sharpness in the slitting of
647 plastic films. *Journal of Materials Science* 31 (5): 1327-1334
- 648 [36] Key, A.J.M. and Lycett, S.J. 2014. Are bigger flakes always better? An
649 experimental assessment of flake size variation in cutting efficiency and loading.
650 *Journal of Archaeological Science* 41: 140-146
- 651 [37] Schuldt S., Arnold G., Roschy J., Schneider Y., and Rohm H. 2013. Defined
652 abrasion procedures for cutting blades and comparative mechanical and geometrical
653 wear characterization. *Wear* 300(1-2): 38-43
- 654 [38] Theriault DH, Fuller NW, Jackson BE, Bluhm E, Evangelista D, Wu Z, Betke
655 M, and Hedrick TL. 2014. A protocol and calibration method for accurate multi-
656 camera field videography. *Journal of Experimental Biology* 217:1843-1848
- 657 [39] Abdel-Aziz YI, and Karara HM. 1971. Direct linear transformation from
658 comparator coordinates into object space coordinates in close-range photogrammetry.
659 *Symposium on Close Range Photogrammetry*. Falls Church, VA: American Society
660 of Photogrammetry. p 1-18
- 661 [40] Hedrick TL. 2008. Software techniques for two- and three-dimensional
662 kinematic measurements of biological and biomimetic systems. *Bioinspiration*
663 *Biomimetics* 3(3):034001
- 664 [41] Wobbrock JO, Findlater L, Gergle D, and Higgins JJ. 2011. The aligned rank
665 transform for nonparametric factorial analyses using only anova procedures. New
666 York, New York, USA: ACM. p 143-146
- 667 [42] Benjamini Y, and Hochberg Y. 1995. Controlling the false discovery rate: a
668 practical and powerful approach to multiple testing. *J R Stat Soc, Ser B*:289-300
- 669 [43] Stafford J.V. 1981. An application of critical stress soil mechanics: the
670 performance of rigid tines. *Journal of Agricultural Engineering Research* 26 (5): 387-
671 401

672

673

674 **Figures**

675



676

677

678

679

680

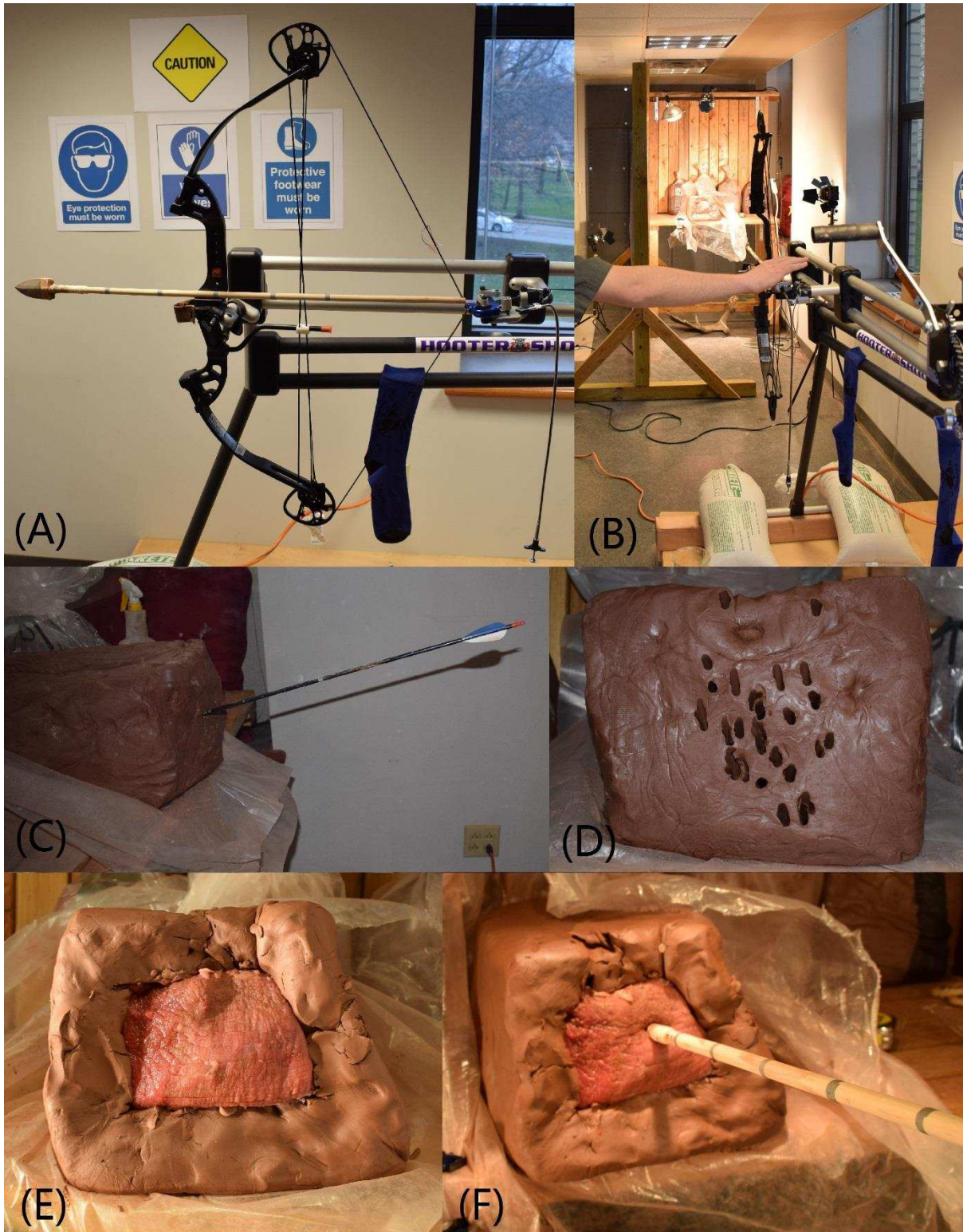
681

682

683

684

Figure 1: Images identifying the Instron® tensile testing machine and experimental set-up when cutting the clay and meat. Images B and C depict blade placement at the start of each cutting test, D and E depict material deformation prior to fracture for the meat (E) and the lack therefore for the clay (D). Images F and G show segments of each material after they have been cut. In clay (F), it is clear that no deformation prior to fracture occurs when the cut is initiated, however, there is potential for marginal material tearing as the blade edge exits. The meat segment (G) was not included in the data sample but highlights the potential for connective tissues to alter the resistance provided by ‘meat’ relative to muscle fibres.



685

686 **Figure 2:** Images identifying the composite bow (A) and projectile range (B) used during this
687 experiment. The clay (C and D) and meat (E and F) targets are also detailed, as are an arrow
688 (C) and stone point (F) after having been fired at the target. Note the reflective tape markers
689 spaced along the length of the projectiles' shafts.



690

691 **Figure 3:** The composite arrow and stone point projectiles used in the penetration
692 experiments. The scale bar is 10cm long in all instances.

693

694

695

696

697

698

699

700

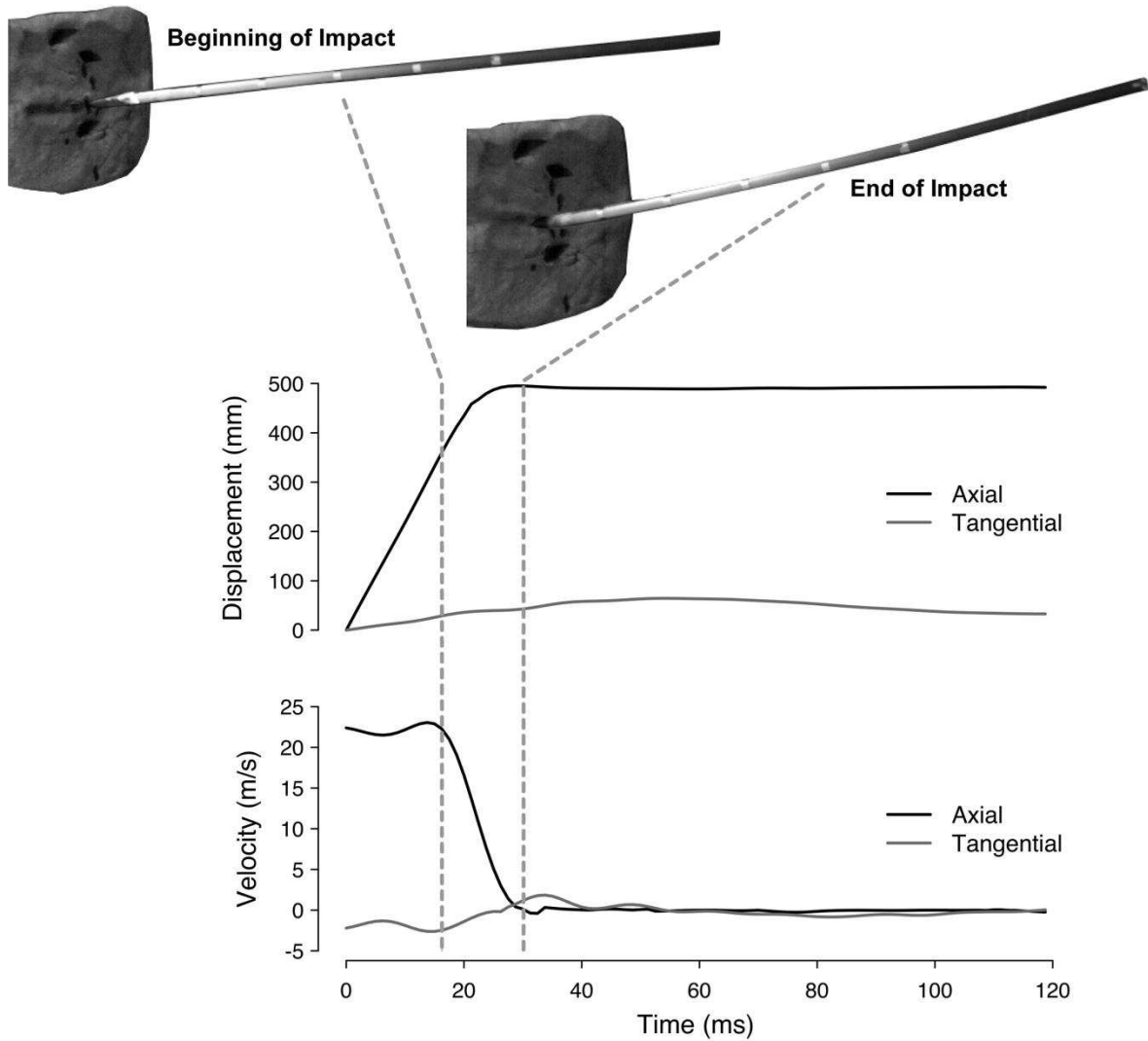
701

702

703

704

705



706

707 **Figure 4:** Kinematics of a projectile impact. An exemplar trial of the stone point impacting
 708 the clay target is illustrated, with graphs showing instantaneous changes in axial and
 709 tangential displacement and velocity during the period of impact. The images at the top were
 710 rendered from the high-speed video and digitally enhanced and cropped to better illustrate
 711 impact events ('mm' = millimetres, 'm/s' = meters per second, 'ms' – milliseconds).

712

713

714

715

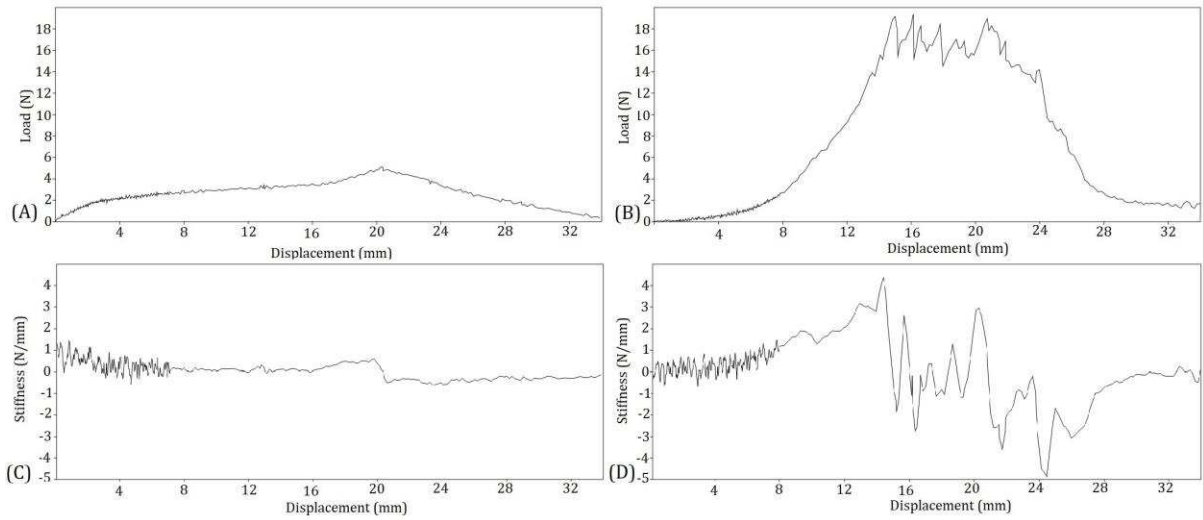
716

717

718

719

720



721

722 **Figure 5:** Load-displacement curves during the clay (A) and meat (B) cutting tests ('N' =
 723 newtons). The corresponding stiffness-displacement curves for clay (C) and meat (D) are also
 724 depicted.

725

726

727

728

729

730

731

732

733

734

735

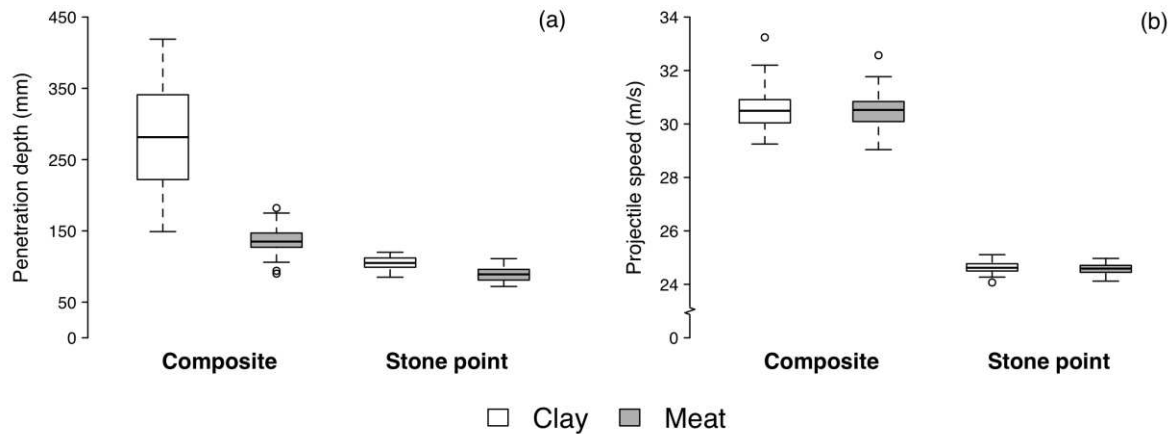
736

737

738

739

740



741

742 **Figure 6:** Box-and-whisker plots of variation in projectile penetration depths and speed, as a
 743 function of projectile and material type during the high-speed camera tests ('mm' =
 744 millimetres, 'm/s' = meters per second). In each plot, bold lines indicate the median of the
 745 distribution, boxes extend to the 1st and 3rd quartiles, and whiskers extend to the most
 746 extreme data points that are no more than $\pm 150\%$ of the interquartile range. Outliers beyond
 747 this range are indicated by individual symbols.

748

749

750

751

752

753

754

755

756

757

758

759

760

761

762

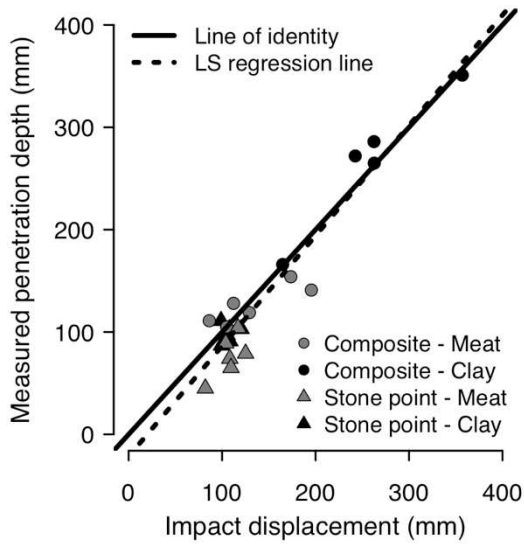
763

764

765

766

767



768

769 **Figure 7:** Validation of motion-tracking analyses of projectile dynamics. Measured
770 penetration depths are plotted against axial projectile displacement during the period of
771 impact ('mm' = millimetres).

772

773

774

775

776

777

778

779

780

781

782

783

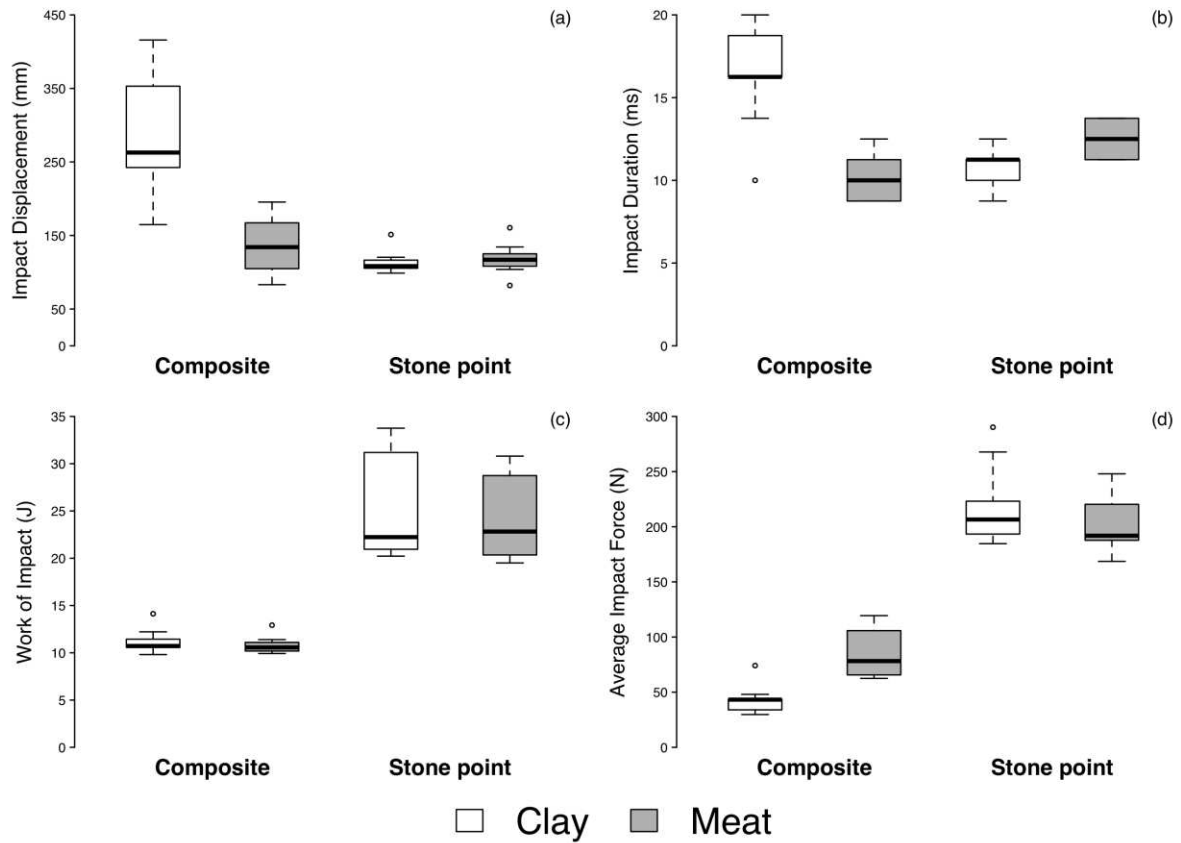
784

785

786

787

788



789

790 **Figure 8:** Box-and-whisker plots of variation in projectile impact dynamics, as a function of
 791 projectile and material type ('mm' = millimetres, 'ms' = milliseconds, 'J' = joules, 'N' =
 792 newtons). In each plot, bold lines indicate the median of the distribution, boxes extend to the
 793 1st and 3rd quartiles, and whiskers extend to the most extreme data points that are no more
 794 than $\pm 150\%$ of the interquartile range. Outliers beyond this range are indicated by individual
 795 symbols.

796

797

798

799

800

801

802

803

804

805

806

807

808 **Tables**

809

810 **Table 1:** Summary high-speed video measurements of projectile impact dynamics.

Variable	Definition
Impact displacement	Axial distance in centimetres (cm) traversed by the projectile during the period of impact.
Impact duration	Time in milliseconds (ms) between the start of projectile deceleration and the cessation of motion.
Work of impact	Work in Joules (J) performed by the target in stopping the projectile – or, equivalently, work performed by the projectile in penetrating the target. Equal to the change in the kinetic energy of the projectile during the duration of impact, where kinetic energy was calculated as one-half the product of projectile mass and the square of instantaneous projectile velocity.
Average force of impact	Average force in Newtons (N) required to arrest projectile motion – equivalent to “stopping power”. Calculated as work of impact divided by impact displacement.

811

812

813

814

815

816

817

818

819

820

821

822

823

824

825

826

827

828

829 **Table 2:** Descriptive loading data for the two raw materials analysed during the cutting tests
830 (n = 30 in all instances). ‘Mean Load’ refers to the average load recorded across a single
831 cutting test (‘N’ = newtons, ‘S.D.’ = standard deviation, ‘C.V.’ = coefficient of variation).

Trial	Clay		Meat	
	Max. Load (N)	Mean Load (N)	Max. Load (N)	Mean Load (N)
Mean	5.2	2.6	16.3	5.8
Minimum	4.1	2.0	8.7	2.2
Maximum	7.1	3.3	25.9	11.8
S.D.	0.7	0.3	4.5	1.7
C.V.	13.3	12.0	27.9	29.8

832
833
834
835
836
837
838
839
840
841
842
843
844
845
846
847
848
849
850
851
852
853
854

855 **Table 3:** Descriptive data detailing the primary penetration depth and speed data of the
 856 composite arrows and stone points when fired into clay and meat ('mm' = millimetres, 'm/s'
 857 = meters per second, 'S.D.' = standard deviation, 'C.V.' = coefficient of variation).

		Composite Arrows (n = 204)		Stone Points (n = 60)	
		Meat (n=102)	Clay (n=102)	Meat (n=30)	Clay (n=30)
Penetration (mm)	Mean	137.3	281.4	88.8	104.8
	S.D.	17.2	73.6	10.2	8.8
	C.V.	12.6	26.2	11.5	8.4
Speed (m/s)	Mean	30.5	30.5	24.6	24.6
	S.D.	0.6	0.6	0.2	0.2
	C.V.	2.1	2.1	0.8	0.9

858
 859
 860
 861
 862
 863
 864
 865
 866
 867
 868
 869
 870
 871
 872
 873
 874
 875
 876
 877
 878
 879
 880
 881

882 **Table 4:** Aligned rank-transformed analyses of variance of the penetration depths, speed and
 883 projectile dynamics of the composite arrows and stone points when fired into clay and meat
 884 ('mm' = millimetres, 'm/s' = meters per second, 'J' = joules, 'N' = newtons).

		Projectile	Material	Interaction	Post-hoc tests
Penetration depth (mm)	F-value	284.6	381.0	100.4	Composite: U = 10301.5, p < 0.001 Stone point: U = 790.5, p < 0.001
	Degrees of freedom	1, 260	1, 260	1, 260	
	p-value	< 0.001	< 0.001	< 0.001	
Speed (m/s)	F-value	289.6	0.04	0.08	NA
	Degrees of freedom	1, 260	1, 260	1, 260	
	p-value	< 0.001	0.846	0.778	
Impact Displacement (mm)	F-value	42.5	30.9	33.0	Composite: U = 87, p < 0.001 Stone point: U = 30, p = 0.39
	Degrees of freedom	1, 33	1, 33	1, 33	
	p-value	< 0.001	< 0.001	< 0.001	
Impact Duration (ms)	F-value	3.5	24.3	44.6	Composite: U = 85.5, p = 0.002 Stone point: U = 16, p = 0.027
	Degrees of freedom	1, 33	1, 33	1, 33	
	p-value	0.07	< 0.001	< 0.001	
Work of Impact (J)	F-value	99.6	0.9	0.2	N/A
	Degrees of freedom	1, 33	1, 33	1, 33	
	p-value	< 0.001	0.348	0.673	
Average Impact Force (N)	F-value	99.7	20.3	17.2	Composite: U = 5, p = 0.003 Stone point: U = 52, p = 0.331

885
 886
 887
 888
 889
 890
 891
 892

893 **Table 5:** High-speed video analyses of projectile impact dynamics ('mm' = millimetres,
 894 'm/s' = meters per second, 'ms' = milliseconds, 'J' = joules, 'N' = newtons, 'S.D.' = standard
 895 deviation, 'C.V.' = coefficient of variation).

		Composite Arrows (n = 19)		Stone Points (n = 18)	
		Meat (n=10)	Clay (n=9)	Meat (n=9)	Clay (n=9)
Peak Axial Speed (m/s)	Mean	34.0	34.8	23.2	23.5
	S.D.	1.24	1.85	1.67	2.39
	C.V.	3.65	5.32	7.20	10.20
Impact Displacement (mm)	Mean	135.4	280.8	118.2	113.3
	S.D.	38.74	79.83	21.83	15.92
	C.V.	28.61	28.43	18.47	14.05
Impact Duration (ms)	Mean	10.0	16.2	12.4	10.8
	S.D.	1.32	3.00	1.16	1.25
	C.V.	13.20	18.50	9.35	11.60
Work of Impact (J)	Mean	10.8	11.2	24.0	24.9
	S.D.	0.90	1.33	4.54	5.71
	C.V.	8.33	11.90	18.90	22.90
Average Impact Force (N)	Mean	85.1	42.7	204.0	220.0
	S.D.	22.6	13.4	25.4	36.1
	C.V.	26.6	31.4	12.5	16.4

896

